

A Dynamic Framework for Intelligent Control of River Flooding - A Case Study

Arturo S. Leon, P.E., M.ASCE¹, Elizabeth A. Kanashiro²,
Rachelle Valverde³ and Venkataramana Sridhar, P.E., M.ASCE⁴

ABSTRACT

This paper presents a case study on the application of a dynamic framework for the intelligent control of flooding in the Boise River system in Idaho. This framework couples a robust and numerically efficient hydraulic routing approach with the popular multi-objective Non-dominated Sorting Genetic Algorithm II (NSGA-II). The novelty of this framework is that it allows for controlled flooding when the conveyance capacity of the river system is exceeded or is about to exceed. Controlled flooding is based on weight factors assigned to each reach of the system depending on the amount of damage that would occur, should a flood occur. For example, an urban setting would receive a higher weight factor than a rural or agricultural area. The weight factor for a reach doesn't need to be constant as it can be made a function of the flooding volume (or water stage) in the reach. The optimization algorithm minimizes flood damage by favoring low weighted floodplain areas (e.g., rural areas) rather than high weighted areas (e.g., urban areas) for the overbank flows. The proposed framework has the potential to

¹Assistant Professor, School of Civil and Construction Engineering, Oregon State University, 220 Owen Hall, Corvallis, OR 97331-3212, USA. E-mail: arturo.leon@oregonstate.edu (Corresponding author)

²Hydraulic Engineer, Ausenco-Vector, Calle Esquilache 371, San Isidro, Lima - Perú. E-mail: Akemi.Kanashiro@ausenco.com

³Graduate Research Assistant, School of Civil and Construction Engineering, Oregon State University, 220 Owen Hall, Corvallis, OR 97331, USA. E-mail: valverdr@onid.orst.edu

⁴Assistant Professor, Civil Engineering, Boise State University, 1910 University Drive, Boise, ID 83725-2060, USA. E-mail: VSridhar@boisestate.edu

improve water management and use of flood-prone areas in river systems, especially of those systems subjected to frequent flooding. This work is part of a long term project which aims at developing a reservoir operation model that combines short-term objectives (e.g., flooding) and long-term objectives (e.g., hydropower, irrigation, water supply). The scope of this first paper is limited to the application of the proposed framework to flood control. Results for the Boise River system show a promising outcome in the application of this framework for flood control.

Keywords: Flooding; Genetic Algorithms; Hydraulic routing; Multi-objective Optimization; Real-time control; Regulated river systems; River management; River operation

List of Figures

1	Flow chart of OSU Rivers	25
2	Cross-section schematic for definition of left and right flooding volumes.	26
3	An example of a Flooding Performance Graph (FPG)	27
4	An example of a Rating performance Graph (RPG)	28
5	Schematic of a river reach	29
6	Schematic of a node	30
7	Schematic of the Boise River's Plan View	31
8	Inflow hydrograph (SWAT) at the Lucky Peak Reservoir in the Boise River Basin for the period between Nov 2041 and August 2042	32
9	Plan view of major storage reservoirs in the Boise River basin.	33
10	Inflow hydrograph subtracting active storage capacity of Anderson Ranch, Arrow Rock, Hubbard reservoirs and Lake Lowell.	34
11	Stage-storage relationship of Lucky Peak reservoir.	35
12	Aerial view of Lucky Peak reservoir and associated structures (source: http://commons.wikimedia.org)	36

13	Rating curve at most downstream end of river system (node J26). . . .	37
14	Flow hydrographs at downstream end of reach R1 for simulated scenarios.	38
15	Flow hydrographs at downstream end of reach R10 for simulated scenarios.	39
16	Detail A in Figure 15.	40
17	Flow hydrographs at downstream end of reach R22 for simulated scenarios.	41
18	Stage hydrographs at downstream end of reach R1 for simulated scenarios.	42
19	Stage hydrographs at downstream end of reach R10 for simulated scenarios.	43
20	Detail B in Figure 19.	44
21	Stage hydrographs at downstream end of reach R22 for simulated scenarios.	45
22	Peak flow at downstream end of reaches R1, R10 and R22 for the second scenario.	46
23	Flooding objective (Eq. 1) for simulated scenarios.	47
24	Inflow, outflow and water stage hydrographs at the Lucky Peak reservoir.	48
25	Gate operation traces (six gates) at the Lucky Peak reservoir according to OSU Rivers	49

INTRODUCTION

River flooding is a recurrent threat that normally ensues a huge cost, both in terms of human suffering and economic losses associated with damage to infrastructure, loss of business, and the cost of insurance claims. From 2005 to 2009 the National Weather Service (2009) estimated 63 billion dollars in losses in the U.S. associated with flood-

ing. The catastrophic disasters associated with river flooding urge the re-evaluation of current strategies for flood control for most appropriate frameworks.

Recent studies on flood mitigation indicate that major emphasis must be given to flood control projects under the greater framework of basin-wide ecosystem rehabilitation (e.g., United Nations Environment Programme 2003, De Bruijn et al. 2008). These studies also aim for improving structural measures for minimizing the impact of floods while emphasizing the importance of risk management in flood control projects. A review of common structural measures used for flood control (e.g., levees, dams) reveals most of these measures are passive (static), with dams being the most important structural measure for flood control (e.g., Wei and Hsu 2008). Most dams built for flood control have gates that are operated based on rule curves, which are determined based on annual estimates of system loads, reservoir storages and resources provided by stakeholders. Rule curves neglect the flow dynamics in the entire river system, which makes this approach a “slow-response” method for flood control. This is particularly true in complex river systems when parts of the river system may have enough in-line storage capacity, while other portions of the system may be overflowing.

A flooding process may be highly dynamic and may start from anywhere in the river system (Leon and Kanashiro 2010). It may start from upstream (e.g., large inflows), downstream (i.e., high water levels at downstream), or laterally from the connecting reaches (e.g., water levels at river junctions near the reach banks). It may change for the same river system depending on inflows to the river system and antecedent boundary conditions. Accounting for system flow dynamics is also important because flow conveyance from one reservoir to another is not instantaneous but depends on the capacity of the connecting reaches, the capacity of associated gates, outlet structures and the dynamic hydraulic gradients. Clearly, rule curves are insufficient for making system-wide operational decisions.

Various models for reservoir operation are available. These include optimization models, simulation models, and combined simulation-optimization models. For achieving an optimal system-wide operational decision for flood control, it was recognized that optimization and simulation components must be combined (e.g., Hydrologic Engineering Center 2003). Within the category of models that combine simulation and optimization, there are various models intended for reservoir operation including flood control. One of these models is the “Generalized Real-Time Flood Control System Model” (Eichert and Pabst 1998) that was developed by the Hydrologic Engineering Center (HEC). Currently, HEC supports three individual reservoir modeling tools for the simulation and optimization of reservoir system operations (Hydrologic Engineering Center 1996, 2003). The tools include: 1) Reservoir Simulation (HEC-ResSim), 2) Multi-Objective Reservoir Optimization (Prescriptive Reservoir Model, HEC-PRM), and 3) Reservoir Flood Control Optimization (HECFloodOpt). HEC-ResSim is a reservoir simulation model that makes operation decisions following the user specified operating rules or guidelines. HEC-PRM and HEC-FloodOpt are optimization models that make operation decisions to maximize system objectives and values as defined by the user. HEC combines these three modeling tools into one package, the Reservoir Evaluation System (HEC-RES). The simulation component of HEC-RES, ResSim, is used extensively in real-time water control as part of the Corps Water Management System (CWMS). The RIBASIM (RIver BASin SIMulation) [Delft Hydraulics 2000] model is another comprehensive and flexible tool for reservoir operation.

Recently, many more combined simulation-optimization models were formulated for reservoir operation including flood control. Ngo et al. (2007) proposed to optimize the control strategies for the Hoa Binh reservoir operation. The control strategies were set up in the MIKE 11 simulation model to guide the releases of the reservoir system

according to the current storage level, the hydro-meteorological conditions, and the time of the year. Lee et al. (2009) refined an existing optimization/simulation procedure for rebalancing flood control and refill objectives for the Columbia River Basin for anticipated global warming. To calibrate the optimization model for the 20th century flow, the objective function was tuned to reproduce the current reliability of reservoir refill, while providing comparable levels of flood control to those produced by current flood control practices. After the optimization model was calibrated using the 20th century flow the same objective function was used to develop flood control curves for a global warming scenario.

Even though there is a wide array of models for reservoir operation, the authors are not aware of any framework intended for the operation of a river system when its capacity has exceeded or is about to exceed. Therefore, it would be desirable to have a framework that allows controlled flooding, where areas with the lowest amount of damage would be allowed to flood first and areas with the highest amount of damage would be allowed to flood last to minimize damage accordingly.

This paper presents a case study on the application of a dynamic framework for the intelligent control of flooding in the Boise River system in Idaho. This framework that is under ongoing development was named OSU Rivers as an acronym for *Oregon State University coupled optimization-simulation model for the operation of regulated river systems*. The OSU Rivers framework couples a robust and numerically efficient hydraulic routing approach with the popular multi-objective Non-dominated Sorting Genetic Algorithm II (NSGA-II). The novelty of this framework is that it allows for controlled flooding when the conveyance capacity of the river system is exceeded or is about to exceed. Controlled flooding is based on weight factors assigned to each reach of the system depending on the amount of damage that would occur, should a flood occur. For example an urban setting would receive a higher weight factor than a rural

or agricultural area. The weight factor for a reach doesn't need to be constant as it can be made a function of the flooding volume (or water stage) in the reach. The optimization algorithm minimizes flood damage by favoring low weighted floodplain areas (e.g., rural areas) rather than high weighted areas (e.g., urban areas) for the overbank flows. In an actual river system, presumably, rural areas are already more prone to flooding (flood more frequently), because of existing planning and land management practices. However, the proposed framework has the potential to refine and improve water management and use of flood-prone areas in river systems, especially of those systems subjected to frequent flooding.

The work presented here is part of a long term project, which overarching goal is the development of a reservoir operation model that combines short-term objectives (e.g., flooding) and long-term objectives (e.g., hydropower, irrigation, water supply). The scope of this first paper is limited to the application of OSU Rivers to flood control (short-term objective). The treatment of long-term objectives will be described in a subsequent paper. This paper is organized as follows: (1) the optimization and simulation components of OSU Rivers are briefly described; (2) a concise description of the river system routing of OSU Rivers is presented; (3) the model is applied to the Boise River system in Idaho. Finally, the results are summarized in the conclusion.

COMPONENTS OF THE PROPOSED FRAMEWORK

The proposed framework, the flow chart of which is presented in Figure 1, is essentially a real-time operational model that links two components: optimization and river system routing (simulation).

Optimization component: The Non-dominated Sorting Genetic Algorithm-II (NSGA-II)

The optimization component of the OSU Rivers framework uses the popular Non-dominated Sorting Genetic Algorithm-II (NSGA-II), which has been chosen based on

its recent successful implementation in reservoir optimization analysis (e.g., Kim et al. 2006). The NSGA-II algorithm has been shown to be one of the most efficient algorithms for multi-objective optimization on a number of benchmark problems, including water resources engineering problems (e.g., Bekele and Nicklow 2007). Some of the recent applications to water resources engineering include multi-reservoir system optimization (e.g., Kim et al. 2006), optimal design of water distribution networks (Atiquz-zaman et al. 2006), long-term groundwater monitoring design (Reed and Minsker 2004), and watershed water quality management (Dorn and Ranji-Ranjithan 2003). The main features of these algorithms are the implementation of a fast non-dominated sorting procedure and its ability to handle multiple objectives simultaneously without weight factors.

The reason for choosing a multi-objective optimization technique (i.e., NSGA-II) is that, under non-flooding conditions, the OSU Rivers framework maximizes the benefits of the river system that may be multi-objective such as hydropower production, irrigation and water supply. Under flooding conditions, the OSU Rivers framework uses a single-objective (minimize flooding), however to avoid using different algorithms, the multi-objective NSGA-II technique is used for both flooding and non-flooding conditions.

Simulation component

The hydraulic component of the proposed framework consists of dividing the river system into reaches and pre-computing the hydraulics for each of these reaches independently using any gradually varied flow model (one-, two- or three-dimensional model). The pre-computed hydraulics for each reach is stored in matrices and is accessed as look up tables. The hydraulic routing adopted for each river reach is performed using the Hydraulic Performance Graph (HPG) and Volume Performance Graph (VPG). The HPG of a channel reach graphically summarizes the dynamic rela-

tion between the flow through and the stages at the ends of the reach under gradually varied flow (GVF) conditions, while the VPG summarizes the corresponding storage. The storage volumes from VPGs are divided into left, right and main channel storages volumes. The left and right inundation volumes are summarized into Left Flooding Performance Graphs (LFPGs) and Right Flooding Performance Graphs (RFPGs), respectively. The LFPGs and RFPGs represent volumes of water outside of levee limits, channel banks or topographic thresholds that were used to define the limits of inundation (See Figure 2). An example of an LFPG is shown in Figure 3.

At the location of in-line structures (controlled and uncontrolled), the proposed framework makes use of Rating Performance Graphs (RPGs). An RPG graphically summarizes the dynamic relation between the flow through and the stages upstream and downstream of an in-line structure under GVF conditions. Figure 4 depicts a typical graph of an RPG. Physical measurements of flow discharge and water stages or numerical simulations using one-, two- or three-dimensional numerical models can be used for constructing RPGs. In OSU Rivers, all internal nodes (uncontrolled and controlled in-line structures and channel junctions) are assumed to have no storage. The water depth immediately upstream of the in-line structure is computed using the RPG constructed for the structure. For a detailed description of the hydraulic component of the proposed framework the reader is referred to Leon et al. (2012).

Description of the proposed framework

For facilitating the description of OSU Rivers, this model can be divided into five modules. These are:

Module I: Representation of a river network

In the proposed model, a river system is represented by river reaches and nodes. A river reach is defined by its upstream and downstream nodes and must have more or less uniform properties along the reach (e.g., cross-section, bed slope). The flow

direction in a river reach is assumed to be from its upstream node to its downstream node as shown in Figure 5. A negative flow discharge in a river reach indicates that reverse flow occurs in that river reach. In Figure 5, the subscript j and superscript n represent the river reach index and the discrete-time index, respectively. Also, y is water depth, Q is flow discharge and the subscripts u and d denote the upstream and downstream ends of a river reach, respectively.

A node, which is depicted schematically in Figure 6, may have v inflowing river reaches and p outflowing river reaches, with $k = v + p$, where k is the total number of river reaches linked to the node. A river reach is denoted as inflowing (or outflowing) when it conveys to (or from) the node. Several types of boundaries conditions (BCs) are supported by the proposed model. A description of these boundaries is presented below.

1. External Boundary Conditions (EBCs), which are prescribed at the most upstream and downstream ends of the river system. EBCs include inflow hydrographs, stage hydrographs or stage-discharge ratings. An EBC can have either an inflowing or outflowing river reach connected to the node but not both.
2. Internal Boundary Conditions (IBCs), which are specified at internal nodes whenever two or more reaches meet. The three types of IBCs currently supported by OSU Rivers are:
 - Uncontrolled in-line structures (e.g., dams without operation of gates, bridges). A single RPG is necessary for these structures.
 - Controlled in-line structures (e.g., gates, rising weirs). An array of RPGs is necessary for this type of structure, one for each discrete gate position so as to encompass the full range of operation of the gate(s). Typically, gates installed in dams are identical and have an equal in-

vert elevation. For instance, if a dam has 10 identical gates that have the same invert elevation, all gates have the same RPG, which reduces drastically the number of RPGs needed for simulations.

- Junctions, which are schematically depicted in Figure 6, represent nodes without presence of hydraulic structures. A junction node is assumed not to have storage and may connect two or more river reaches.

Module II: Computation of HPGs, VPGs, LFPGs, RFPGs and RPGs

HPGs, VPGs, LFPGs, RFPGs are needed for all reaches of the river system, while RPGs are needed for all uncontrolled and controlled in-line structures. The flow discharges used for constructing the performance graphs should range from near dry-bed states to high water stages (e.g., inundation) using appropriate intervals between flow discharges. These intervals are set according to the desired precision by a trial and error process.

Module III: Initial and Boundary Conditions

The initial conditions are downstream water depths and flow discharges at upstream Q_u and downstream Q_d ends of each river reach. To check the consistency of initial conditions, continuity equations and compatibility conditions of water stages are verified for all internal nodes. The boundary conditions are basically the inflows to the river system and rating curves at the downstream ends of a river system. In OSU Rivers, initial and boundary conditions can be continuously updated by real-time measurements in the river system (e.g., water stages). The latter means that any error in inflow discharge predictions at a previous time step will be minimized by real-time measurements of water stages at the next time step (e.g., mass balance will be conserved).

Module IV: Optimization objective under flooding conditions

Under flooding conditions, the following optimization objective is proposed

$$\text{Minimize } f = \sum_{j=1}^{\text{RR}} (w_{L_j} FV_{L_j} + w_{R_j} FV_{R_j}) \quad (1)$$

Where j denotes a river reach, RR is the total number of river reaches, and FV_{L_j} and FV_{R_j} are left and right flooding volume, respectively (see Figure 2). FV_{L_j} and FV_{R_j} are obtained from the corresponding LFPG and RFPG, respectively. w_L (or w_R) is a weight factor assigned to the left (or right) of each reach of the system depending on the amount of damage that would occur, should the left (or right) of the reach flood. In an actual application, weight factors should be determined from a social and economic study based on a hierarchy of losses that would be incurred as a result of flooding. It is worth mentioning that the weight factor for a reach doesn't need to be constant as it can be made a function of the flooding volume (or water stage) in the reach.

Module V: River system hydraulic routing

This module assembles and solves a non-linear system of equations to perform the hydraulic routing of the river system. These equations are assembled based on information summarized in the systems' HPGs, VPGs and RPGs, the reach-wise equation of conservation of mass, continuity and compatibility conditions of water stages at the union of reaches (nodes), and the system boundary conditions. For a detailed description of this hydraulic routing, the reader is referred to Leon et al. (2012).

APPLICATION OF THE PROPOSED MODEL TO THE BOISE RIVER SYSTEM

For demonstration purposes, this model was applied to the Boise River system in

Idaho, the plan view of which is presented in Figure 7. The Boise River system was divided into twenty five river reaches, including three uncontrolled in-line structures, and one controlled in-line structure.

The controlled in-line structure consists of six sluice gates that are assumed to be operated automatically to fulfill the objective of the application. The upstream end of reach R1 is located right downstream of Boise River Diversion Dam and the downstream end of reach R25 is located approximately 2600m downstream near Glenwood bridge.

Hydrologic Modeling

For the inflow to the Boise River system, an inflow hydrograph was obtained using the Soil and Water Assessment Tool (SWAT) for a climate change scenario. For data-limited, complex terrain such as the Boise River basin, this model provides the best approximation of the basin's response to precipitation events. This model has been implemented for other Idaho watersheds earlier (Stratton et al. 2009, Sridhar and Nayak 2010, Jin and Sridhar 2011). The basic drivers for this model are USGS-derived Digital Elevation Model, STATSGO soil layer, National Land Cover Data 2001 for vegetation and weather data. SWAT was used to quantify possible impacts of climate change due to anticipated precipitation and temperature increase as this is expected to cause a significant shift in the timing and magnitude of streamflow.

The climate change scenario used in this application is the IPSL-CM4 from the Institut Pierre Simon Laplace (IPSL), CNRS, CEA, France. This model in general projects a wetter winter for the study region. Based on the Special Report on Emission Scenarios (SRES) illustrative scenario, we chose A1B (750 parts per million CO₂) for deriving temperature and precipitation products. The spatial resolution of this model is $2.5^{\circ} \times 3.75^{\circ}$, however, we have downscaled the climate model-produced temperature and precipitation to 1/8th degree to drive the hydrology model. For details on the

downscaling and SWAT model simulation the readers are referred to Jin and Sridhar (2011). The inflow hydrograph consisting of average daily and natural flows for a fifty year period (from 01/01/2010 to 12/19/2059) was generated at the Lucky Peak Reservoir. This inflow hydrograph represents natural flows, which means that the storage capacity of the Lucky Peak Reservoir and the flow diversions are not considered. For the present application, a period of nine months (274 days) between 11/30/2041 and 08/30/2042 from the fifty year period was selected and used in the simulations. This inflow hydrograph, which is depicted in Figure 8, corresponds to the largest volume of inflow during a period of nine months.

In this region, the snowpack in the higher mountains acts as a natural reservoir, storing precipitation from the preceding winter. Most of this precipitation falls as snow and accumulates, and during the warm season, the snowpacks melt and release water as runoff into the rivers. In the Boise River system the peak flow season starts in the spring and ends in the middle of the summer, from April through July. (Figure 8). Also, Figure 8 shows that during December there is an increasing flow due to precipitation possibly as rain-on-snow, and between January to February and after July, the inflow hydrograph presents low flows. The rain-on-snow events and increasing temperature in the winter are potential triggers for flooding under future climate conditions.

In this application, Anderson Ranch reservoir, Arrow Rock reservoir, Lake Lowell and Hubbard Dam could not be simulated because stage-storage curve of these storage facilities were not available to the authors. Anderson Ranch reservoir and Arrow Rock reservoir are located upstream of the Lucky Peak reservoir (See, Figure 9).

The active storage capacity of Anderson Ranch and Arrow Rock reservoirs are 509.6 and 335.8 million cubic meters (MCM), respectively. In order to consider the active storage capacity of the aforementioned reservoirs, a constant flow discharge of 90 m³/s was subtracted from the inflow hydrograph between 03/07/2042 and 05/11/2042

for filling Anderson Ranch reservoir, while a constant flow discharge of $84 \text{ m}^3/\text{s}$ was subtracted from the inflow hydrograph between 03/25/2042 and 05/10/2042 for filling Arrow Rock reservoir. The Boise River Diversion Dam, an inline structure located downstream of Lucky Peak reservoir and upstream of river reach R1, diverts water into the New York Canal. The New York Canal feeds Lake Lowell (196.6 MCM) and Hubbard Dam (4.9 MCM), presented in Figure 9. The geometry of the Boise River for this application starts downstream of the Boise River Diversion Dam. In order to consider the active storage capacity of Lake Lowell and Hubbard Dam, a constant flow discharge of $51.5 \text{ m}^3/\text{s}$ was subtracted from the inflow hydrograph between 03/18/2042 and 04/30/2042 for filling Lake Lowell, while a constant flow discharge of $10 \text{ m}^3/\text{s}$ was subtracted from the inflow hydrograph between 05/05/2042 and 05/09/2042 for filling Hubbard Dam.

The flow hydrograph resulting from reducing the storage in Anderson Ranch reservoir, Arrow Rock reservoir, Lake Lowell and Hubbard dam is depicted in Figure 10. This flow hydrograph was used as inflow to the river system at node J1 in the present application. The inflow reduction due to filling of the aforementioned storage facilities causes low flow between 03/07/2042 and 05/01/2042. The stage-storage curve for Lucky Peak reservoir is presented in Figure 11.

Optimization objective and constraints

The optimization objective is to minimize flooding according to Eq. 1. Weight factors were assumed to be between one and three. These numbers were chosen for demonstration purposes and are not based on an actual social and economic study. In an actual application, weight factors should be determined from a social and economic study based on a hierarchy of losses that would be incurred as a result of flooding. As mentioned earlier, the weight factor for a reach doesn't need to be constant as it can be made a function of the flooding volume (or water stage) in the reach. A weight factor

of one was assumed for the left and right sides of reaches R1 to R4. Reaches R1 to R4 correspond to the Barber pool conservation area (grasslands). A weight factor of two was assumed for the left side of reaches R5, R6, R16 and R17 and for the right side of reaches R6, R7, R9, R10, R11, R14, R17, R19 and R21. These regions correspond to parks and agricultural areas. Finally, a weight factor of three was assumed for the rest of the river system. These regions correspond to residential, commercial and business areas.

The water stage in the reservoir was constrained to the minimum operating level of 874.5 m. The outflow discharge at the Lucky Peak dam was constrained to the maximum flow discharge of $184 \text{ m}^3/\text{s}$, which is the maximum flow that the Boise River can convey without producing flooding under normal flow conditions. Note that this maximum flow discharge ($184 \text{ m}^3/\text{s}$) corresponds to normal flow conditions (no backwater effects). In unsteady flow conditions, flooding may occur at smaller or larger discharges than that corresponding to the normal flow conditions. The outlet structure of the Lucky Peak reservoir consists of a 6.706 m diameter steel-lined pressure tunnel at the upstream end of the outlet structure and six sluice gates (1.6 m width and 3.048 m height) at the downstream end of the outlet. The hydraulic capacities of the upstream and downstream ends of the outlet structure were compared. The gate conveyance was smaller than that of the tunnel and hence it controls the flow discharge through the outlet structure. The plan view of Lucky Peak reservoir and the associated structures are shown in Figure 12. The characteristics of the river reaches are given in Table 1.

The decision variable used in the optimization is the percentage of opening of the gates in a discrete fashion (discrete optimal control). Thirty two discrete positions (each 10 cm) have been considered for all gates, and all gates were assumed to be operated identically (i.e., same gate invert elevation). The first position corresponded to the gate totally closed and the thirty two position to the gate totally opened. The

use of the opening of the gates as decision variable can be justified in this application because all gates were identical and they were assumed to be operated identically. However, when the inline structure has different controlled hydraulic structures (e.g., gates having different invert elevations), the total flow discharge at the inline structure rather than the percentage of opening of the gates should be used as decision variable. Once the optimized value of the flow discharge at the inline structure is determined, the RPG at the inline structure can be used for determining a combination of gates that satisfy this optimized flow discharge. Clearly, multiple combinations of gates may provide the same flow discharge

Initial and boundary conditions

The system under consideration has two external boundary conditions (EBCs): the first BC is an inflow hydrograph at the upstream end of the Lucky Peak reservoir (see Figure 10) and the second BC is a flow-stage relation at the downstream end of the last river reach (see Figure 13). This flow-stage relation was built assuming critical flow conditions. The initial conditions are a constant flow discharge in the system of $166.7 \text{ m}^3/\text{s}$ and a water stage in the Lucky Peak reservoir of 879.84 m. The simulation time step and the operational decision time used were one hour.

Three scenarios were simulated. The first scenario is with no gate operation, i.e. the gates are closed. The second scenario assumes that the Lucky Peak reservoir does not exist. The third scenario operates the gates according to the results of the proposed framework (minimizing the objective function presented in Eq. 1).

Results and analysis of scenarios

The simulated results for flow and stage hydrographs for the three scenarios under consideration are presented in Figures 14 to 17 and 18 to 21, respectively. Reaches R1, R10 and R22 are located at upstream, downstream and midway of the system (see Figure 7), respectively. In the first scenario the gates remain closed and hence the

reservoir is rapidly filled. As expected, when the reservoir is full, the flow hydrograph downstream of the reservoir (flow over the spillway) is similar to that of the second scenario (no reservoir). The third scenario provides a better control of flooding, however flooding is not entirely avoided due to storage limitations. Figures 16 and 20 show a zoom-in of regions *A* and *B* in Figures 15 and 19 (reach R10), respectively.

To estimate the flood attenuation by the Boise River downstream of Lucky peak reservoir, an enlarged view of peak flows at the downstream ends of reaches R1, R10 and R22 for the second scenario (no reservoir) is presented in Figure 22. The inflow hydrograph is also shown in Figure 22. As can be observed, the peak flow arrives to the downstream end of reaches R1, R10 and R22 after one, three and seven hours, respectively. The attenuation of the peak inflow hydrograph was calculated to be $2.41 \text{ m}^3/\text{s}$ (0.28%), $3.87 \text{ m}^3/\text{s}$ (0.44%) and $6.35 \text{ m}^3/\text{s}$ (0.73%) when the peak flow arrives at the downstream end of reaches R1, R10 and R22, respectively (see Figure 22). This small attenuation is because the storage capacity of the Boise River system downstream of Lucky peak reservoir is very small. The storage capacity of Boise River downstream of the reservoir is about 0.7% of the maximum storage capacity of Lucky peak reservoir.

The simulated results of the flooding objective (Eq. 1) are shown in Figure 23. Results of flooding volume and objective function 1 show that the river starts to flood at day 16 for the first scenario, at day 2 for the second scenario and at day 165 for the third scenario. Note that for the simulated inflow hydrograph, the Boise River would flood for all scenarios. The operation of gates according to the proposed framework (third scenario) attenuates and delays the flood but does not avoid flooding due to lack of sufficient storage capacity. The storage capacity needed to avoid flooding for the inflow hydrograph under consideration is 1,323 MCM. This means that another reservoir with a capacity similar to that of Lucky peak reservoir (about 600 MCM) would be necessary to avoid flooding in this case.

Results for optimized outflow discharges and water stages at the Lucky Peak reservoir according to the proposed framework (third scenario) are presented in Figure 24. Figure 25 shows the corresponding trace of gate openings.

For the third scenario, before the reservoir is full, operated gates release a flow discharge lower than $184 \text{ m}^3/\text{s}$, which is the maximum flow discharge without flooding under normal flow conditions. When the reservoir is full, the flow hydrograph is similar to the inflow hydrograph. The third scenario delayed and better controlled flooding; however, flooding is not entirely avoided due to storage limitations.

CONCLUSIONS

This paper presents a dynamic framework for the intelligent control of river flooding. The novelty of this framework is that it allows for controlled flooding when the conveyance capacity of the river system is exceeded or is about to exceed. The proposed approach links two components: river system routing (simulation) and optimization. The river system routing (simulation) component builds upon the application of Performance Graphs, while the optimization component uses the popular second generation multi-objective evolutionary algorithm Non-dominated Sorting Genetic Algorithm-II (NSGA-II). For illustration purposes, the proposed framework was applied to the Boise River system in Idaho. The key findings are as follows:

1. Results show that the Boise River would flood for all scenarios for the simulated inflow hydrograph. The operation of controlled in-line structures according to the results of the proposed framework delays the occurrence of flooding, but does not avoid it due to lack of sufficient storage capacity in the reservoir.
2. The use of performance graphs for river system routing results in a robust and numerically efficient model as most of the computations for the system routing only involves interpolation steps.

3. Overall, the results show a promising outcome in the application of this model for flood control.

ACKNOWLEDGMENTS

The authors gratefully acknowledge the financial support of NSF Idaho EPSCoR Program and the National Science Foundation under award number EPS-0814387. The first author would like to thank the financial support of the School of Civil and Construction Engineering at Oregon State University. The first author would also like to thank Mrs. Carmen Bernedo of MWH Americas for providing insightful comments during the preparation of the manuscript. The last author would also like to acknowledge the partial support that came from NOAA via the Pacific Northwest Climate Impacts Research Consortium under award number NA10OAR4310218. Last but not least, the authors are indebted to the anonymous reviewers for their insight, constructive criticisms and suggestions on an earlier version of the manuscript.

REFERENCES

- Atiquzzaman, M., Liong, S., and Yu, X. (2006). "Alternative decision making in water distribution network with NSGA-II." *Journal of Water Resources Planning and Management*, 132(2), 122–126.
- Bekele, E. G. and Nicklow, J. W. (2007). "Multi-objective automatic calibration of SWAT using NSGA-II." *Journal of Hydrology*, 341(3-4), 165 – 176.
- De Bruijn, K. and Klijn, F. and Mogahey, C. and Mens, M. and Wolfert, H. (2008). "Long-term strategies for flood risk management: scenario definition and strategic alternative design." *FLOODsite report T14-07-02 Deltares*, Delft Hydraulics, Delft, The Netherlands.
- Delft Hydraulics (2000). *RIBASIM user's manual and technical reference manual*. Delft Hydraulics, Delft, The Netherlands.

- Dorn, J. L. and Ranji-Ranjithan, S. (2003). "Evolutionary multi-objective optimization in watershed water quality management." *EMO*, 692–706.
- Eichert, B. S. and Pabst, A. F. (1998). *Generalized Real-Time Flood Control System Model*. U.S. Army Corps of Engineers, Davis, California.
- Hydrologic Engineering Center (1996). "Developing seasonal and long-term reservoir system operation plans using HEC-PRM." *Report RD-40*, U.S. Army Corps of Engineers, Davis, California, USA.
- Hydrologic Engineering Center (2003). *Hydrologic Engineering Center's Prescriptive Reservoir Model, Program Description*. U.S. Army Corps of Engineers, Davis, California, USA.
- Jin, X. and Sridhar, V. (2011). "Impacts of climate change on hydrology and water resources in the Boise and Spokane River Basins." *Journal of American Water Resources Association*, (in press).
- Kim, T., Heo, J.-H., and Jeong, C.-S. (2006). "Multireservoir system optimization in the Han River basin using multi-objective genetic algorithms." *Hydrol. Process.*, 20, 2057 – 2075.
- Lee, S.-Y., Hamlet, A. F., Fitzgerald, C. J., and Burges, S. J. (2009). "Optimized Flood Control in the Columbia River Basin for a Global Warming Scenario." *Journal of Water Resources Planning and Management*, 135(6), 440–450.
- Leon, A. S. and Kanashiro, E. (2010). "A new coupled optimization-hydraulic routing model for real-time operation of highly complex regulated river systems." Presented in the 2010 Watershed Management Conference: Innovations in Watershed Management Under Land Use and Climate Change.
- Leon, A. S., Kanashiro, E. A., and González-Castro, J. A. (2012). "A fast approach for unsteady flow routing in complex river networks." *J. Hydraul. Eng.*, Under review.
- National Weather Service (2009). "Flood losses: Compilation of flood loss statistics",

<http://www.weather.gov/hic/flood_stats/Flood_loss_time_series.shtml>.

- Ngo, L. L., Madsen, H., and Rosbjerg, D. (2007). "Simulation and optimization modelling approach for operation of the Hoa Binh reservoir, Vietnam." *Journal of Hydrology*, 336(34), 269 – 281.
- Reed, P. M. and Minsker, B. S. (2004). "Striking the balance: Long-term groundwater monitoring design for conflicting objectives." *Journal of Water Resources Planning and Management*, 130(2), 140–149.
- Sridhar, V. and Nayak, A. (2010). "Implications of climate-driven variability and trends for the hydrologic assessment of the Reynolds Creek Experimental Watershed, Idaho." *Journal of Hydrology*, 385(1-4), 183 – 202.
- Stratton, B. T., Sridhar, V., Gribb, M. M., McNamara, J. P., and Narasimhan, B. (2009). "Modeling the spatially varying water balance processes in a semiarid mountainous watershed of Idaho." *Journal of the American Water Resources Association*, 45, 1390–1408 10.1111/j.1752-1688.2009.00371.x.
- United Nations Environment Programme (2003). "Taking it at the flood", <<http://www.unep.org/ourplanet/imgversn/141/shu.html>>.
- Wei, C.-C. and Hsu, N.-S. (2008). "Multireservoir flood-control optimization with neural-based linear channel level routing under tidal effects." *Water Resources Management*, 22, 1625–1647 10.1007/s11269-008-9246-8.

NOTATION

The following symbols are used in this paper:

EBC = external boundary condition;

\bar{c} = average gravity wave celerity;

HPG = hydraulic performance graph;

I = inflow;

$\forall i$ = for all i ;

N = set of nodes;

NB = set of downstream boundary nodes;

NS = set of source nodes;

O = outflow;

Q_{d_j} = flow discharge at downstream end of reach j ;

Q_{u_j} = flow discharge at upstream end of reach j ;

S = storage;

\bar{u} = average reach velocity;

VPG = volume performance graph;

Δx = length of river reach;

y_{d_j} = water depth at downstream end of reach j ;

y_{u_j} = water depth at upstream end of reach j ;

z_{d_j} = channel bottom elevation at downstream end of reach j ;

z_{u_j} = channel bottom elevation at upstream end of reach j ;

Δt = time step

Subscripts

d = downstream end index;

i = node index;

j = river reach index;

u = upstream end index

Superscripts

n = discrete-time index

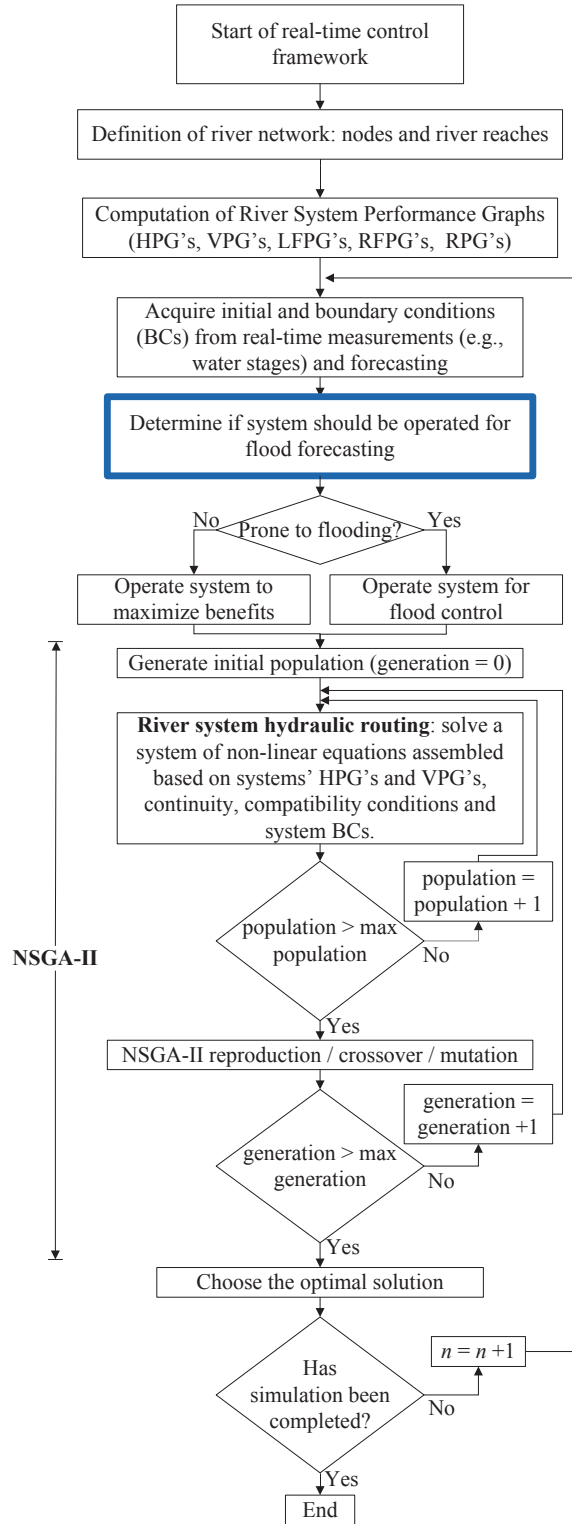


FIG. 1. Flow chart of OSU Rivers

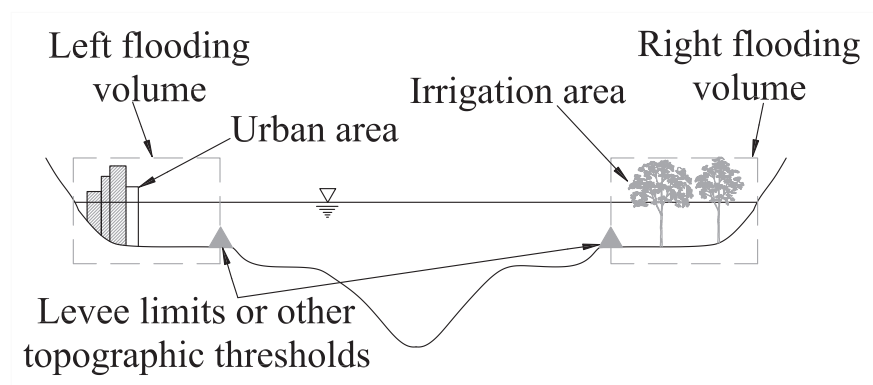


FIG. 2. Cross-section schematic for definition of left and right flooding volumes.

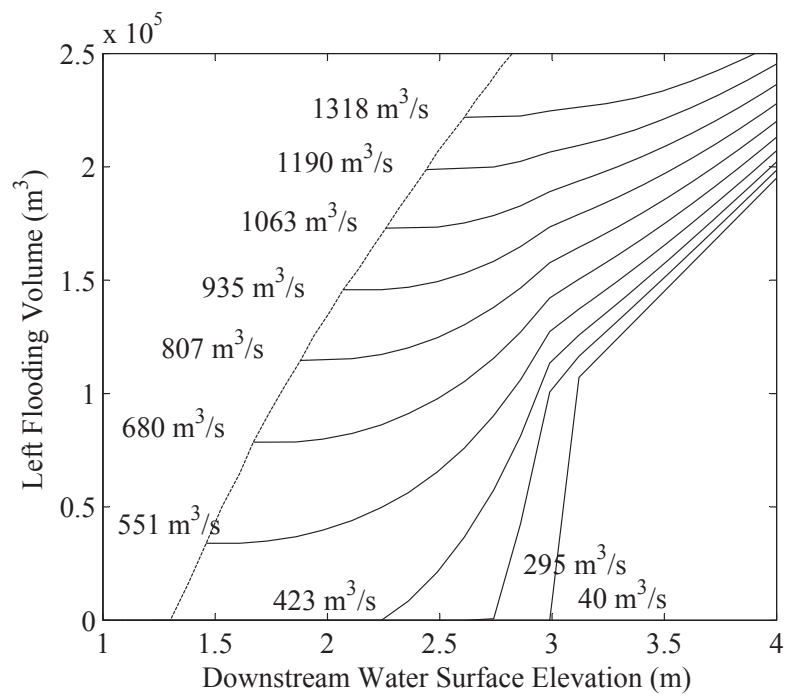


FIG. 3. An example of a Flooding Performance Graph (FPG)

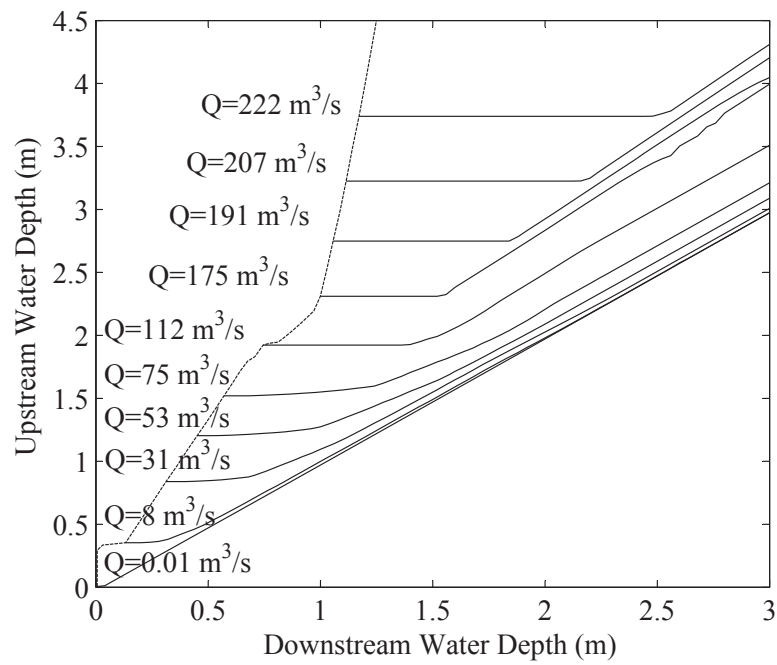


FIG. 4. An example of a Rating performance Graph (RPG)

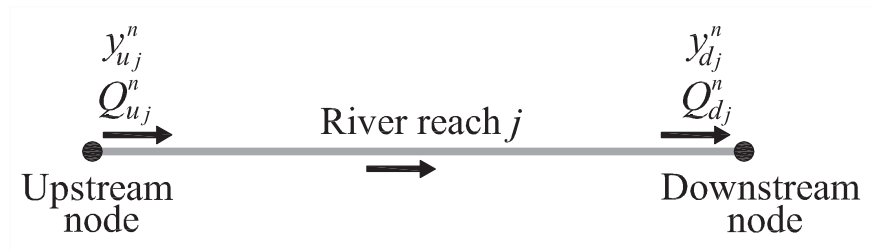


FIG. 5. Schematic of a river reach

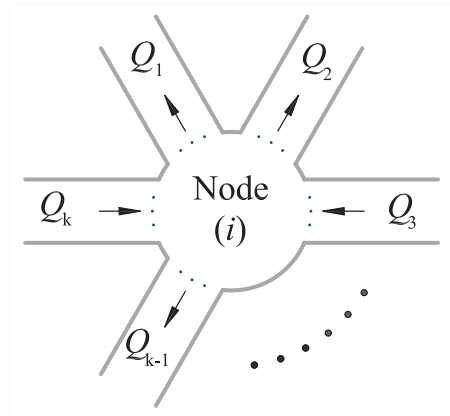


FIG. 6. Schematic of a node

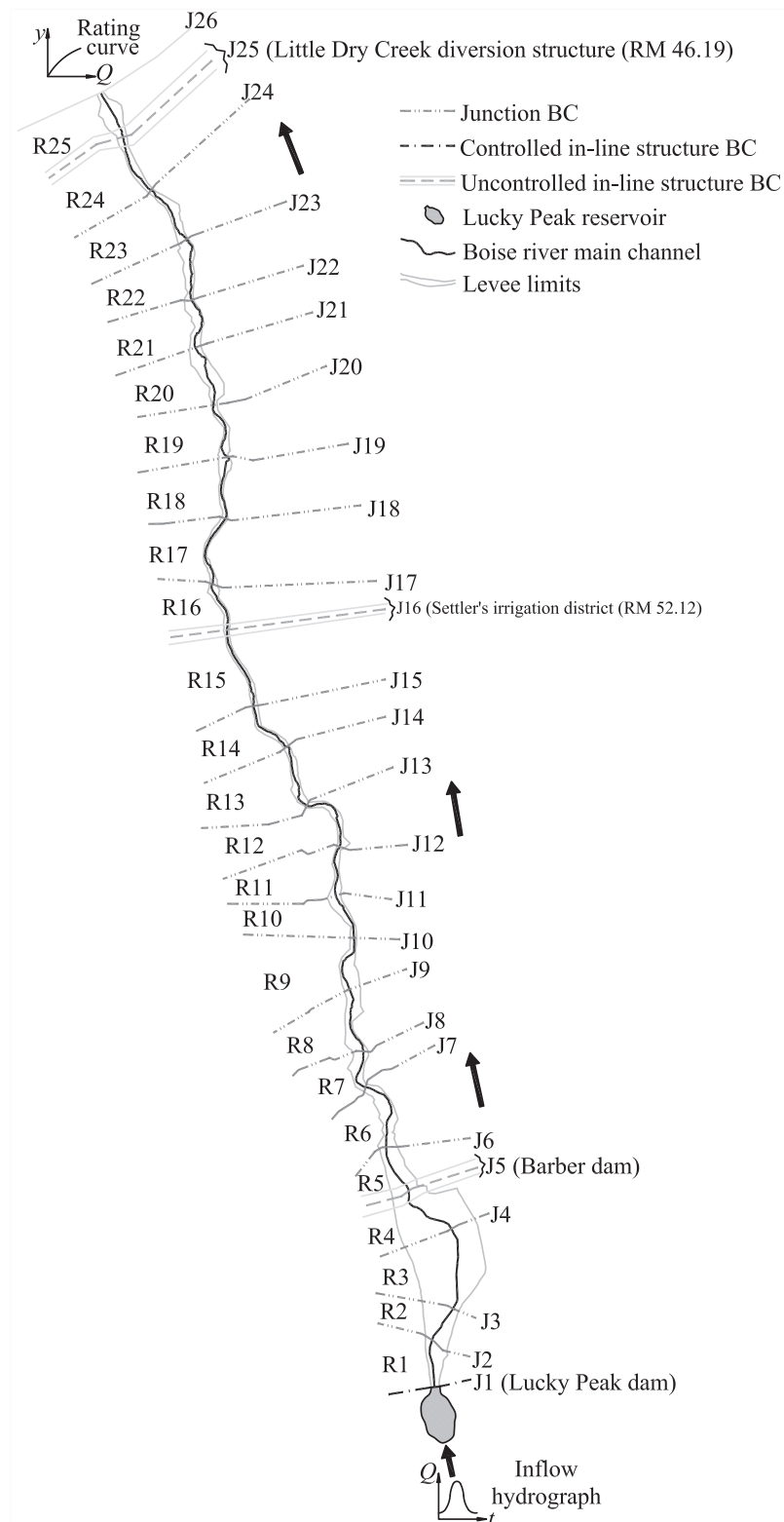


FIG. 7. Schematic of the Boise River's Plan View

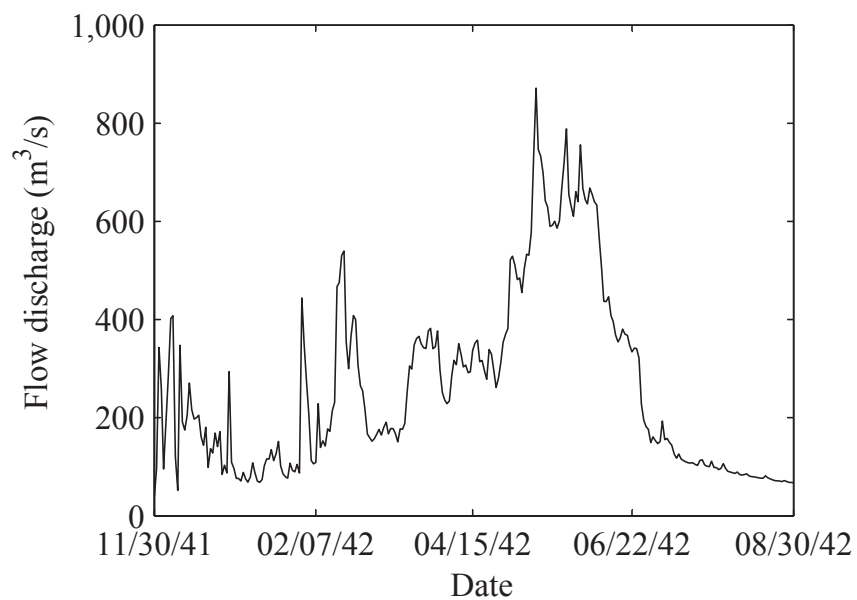


FIG. 8. Inflow hydrograph (SWAT) at the Lucky Peak Reservoir in the Boise River Basin for the period between Nov 2041 and August 2042

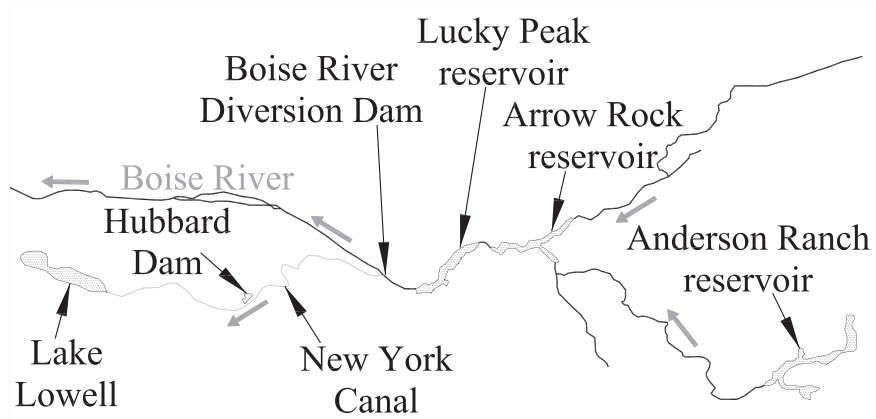


FIG. 9. Plan view of major storage reservoirs in the Boise River basin.

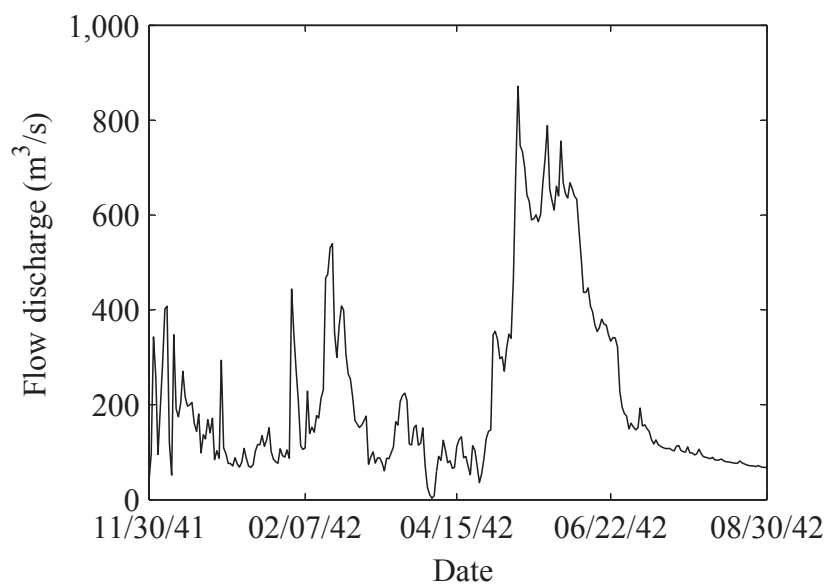


FIG. 10. Inflow hydrograph subtracting active storage capacity of Anderson Ranch, Arrow Rock, Hubbard reservoirs and Lake Lowell.

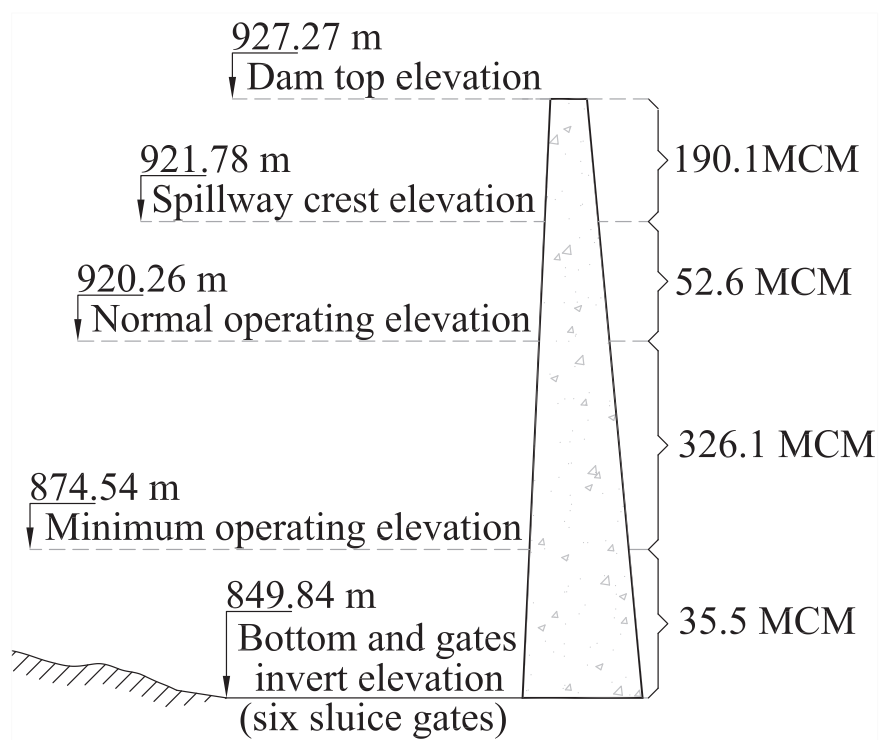


FIG. 11. Stage-storage relationship of Lucky Peak reservoir.

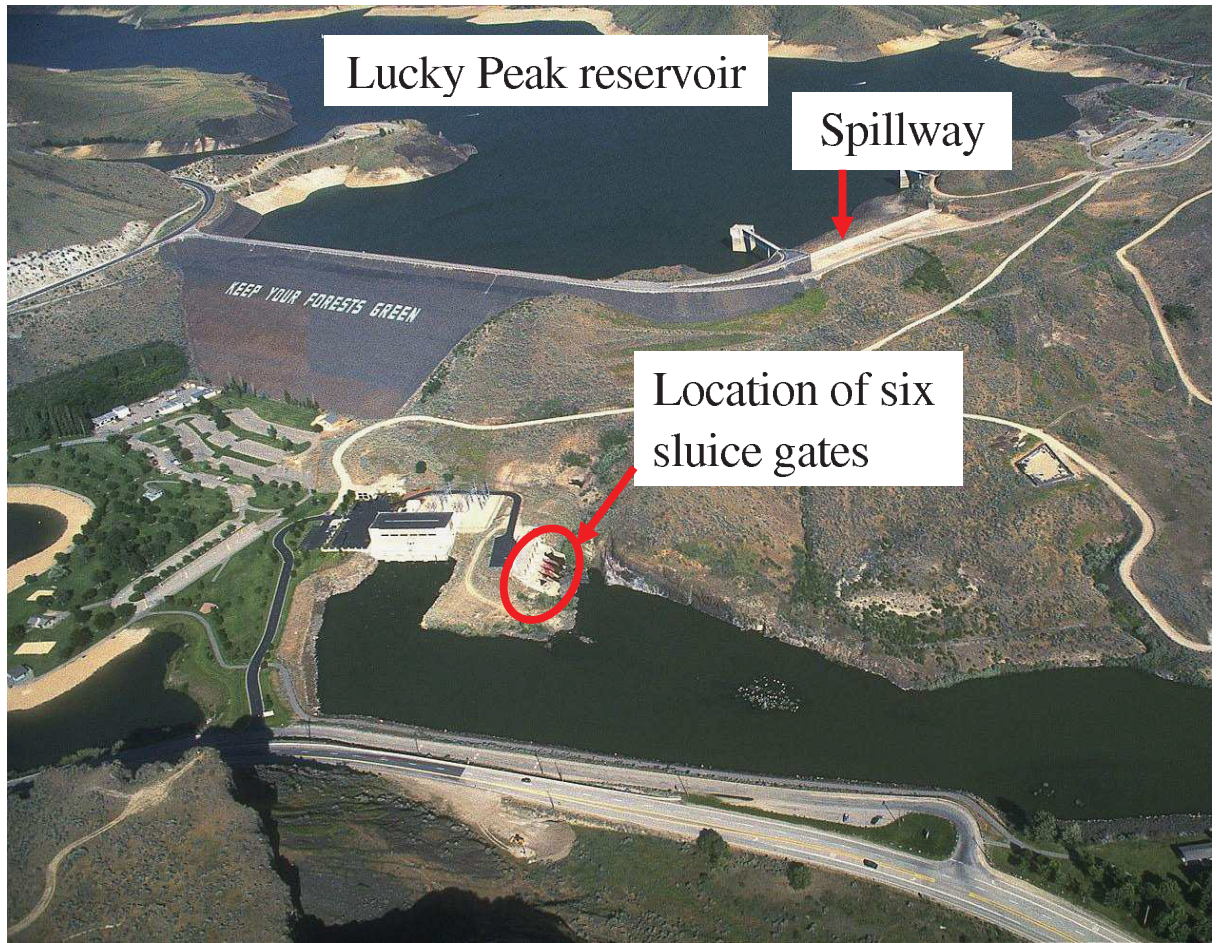


FIG. 12. Aerial view of Lucky Peak reservoir and associated structures
(source: <http://commons.wikimedia.org>)

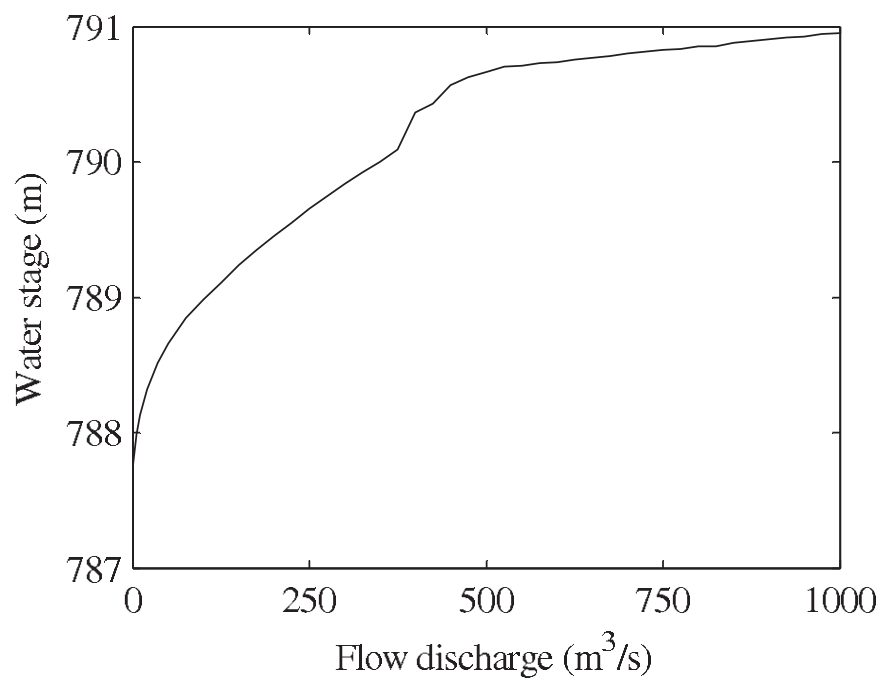


FIG. 13. Rating curve at most downstream end of river system (node J26).

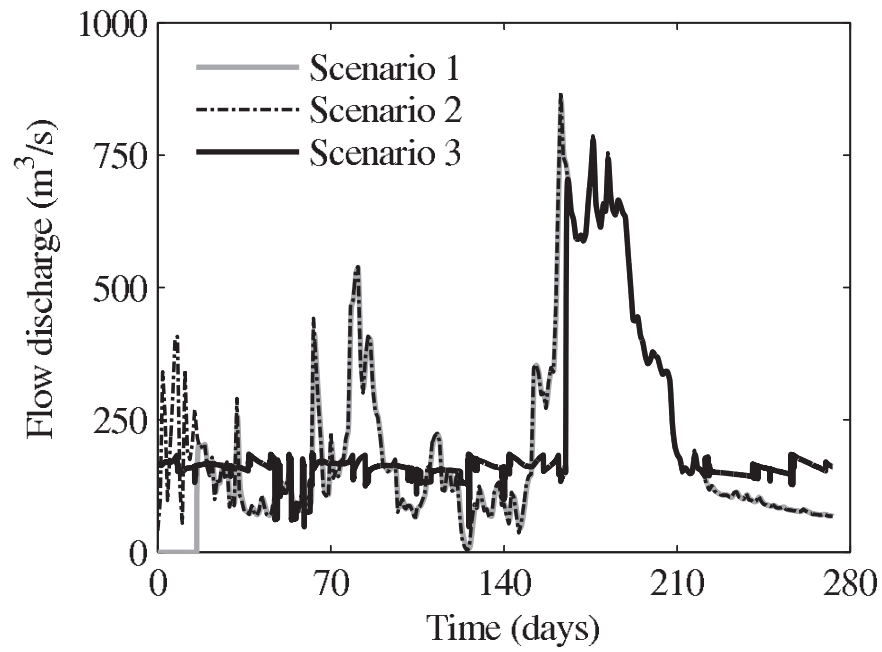


FIG. 14. Flow hydrographs at downstream end of reach R1 for simulated scenarios.

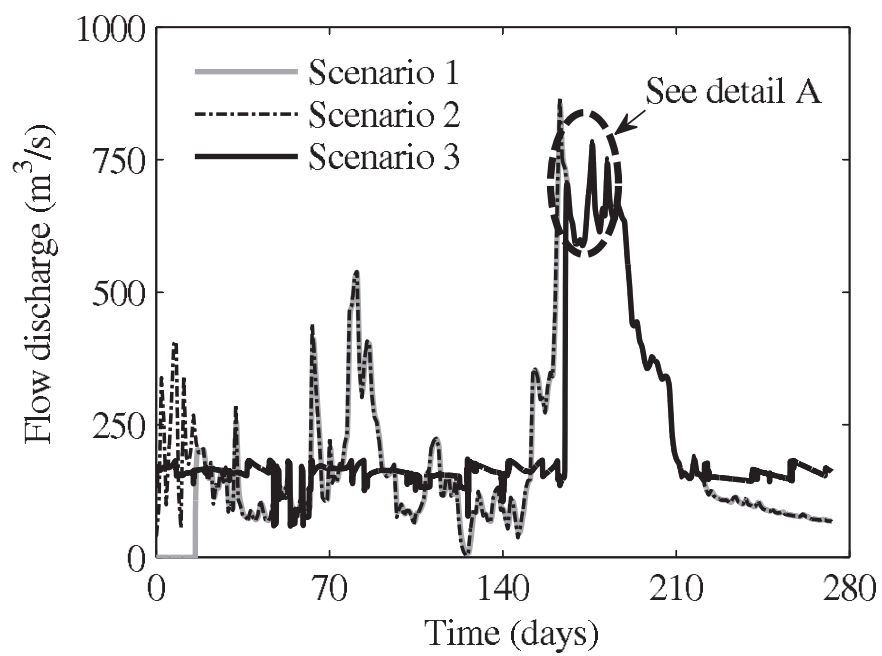


FIG. 15. Flow hydrographs at downstream end of reach R10 for simulated scenarios.

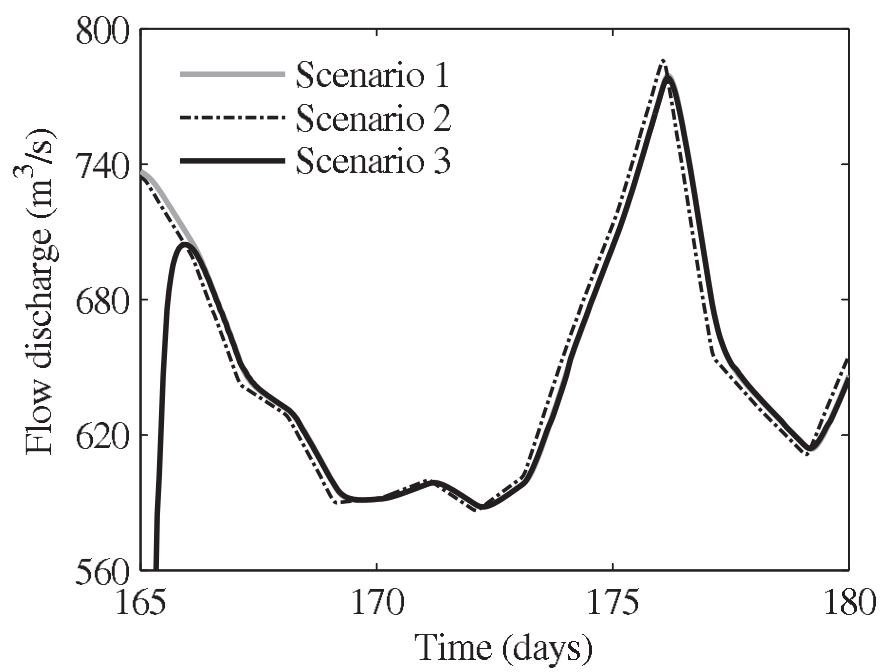


FIG. 16. Detail A in Figure 15.

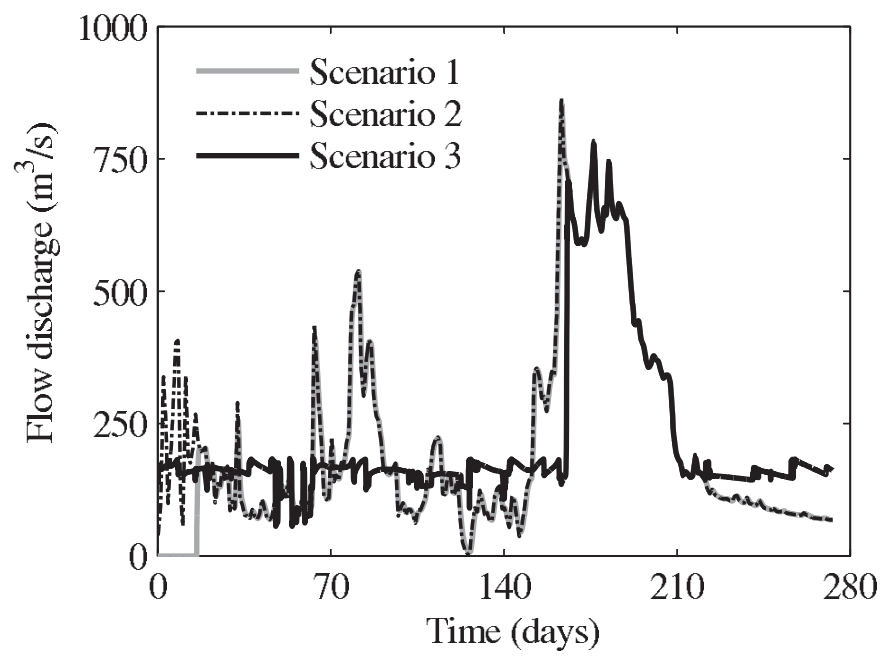


FIG. 17. Flow hydrographs at downstream end of reach R22 for simulated scenarios.

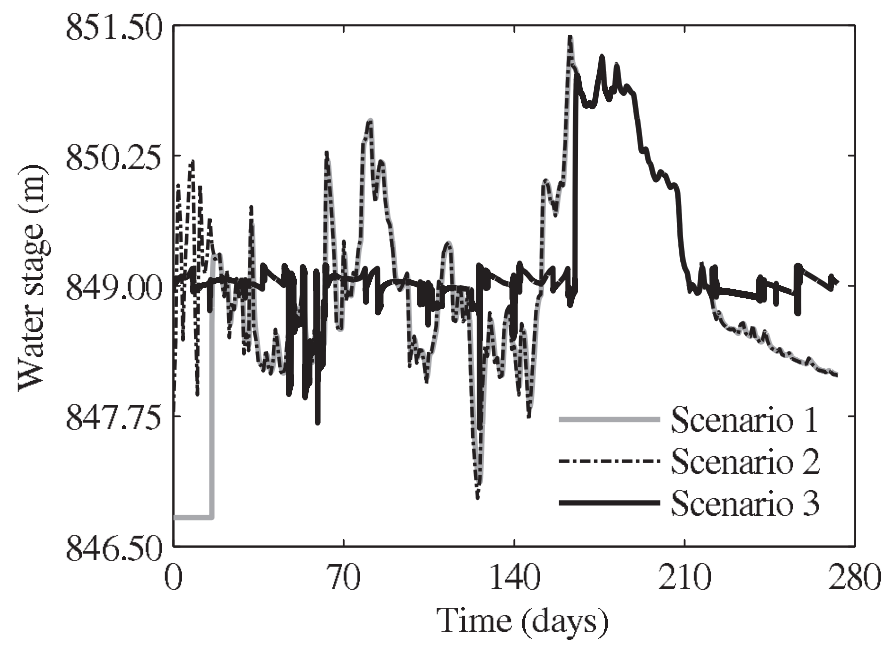


FIG. 18. Stage hydrographs at downstream end of reach R1 for simulated scenarios.

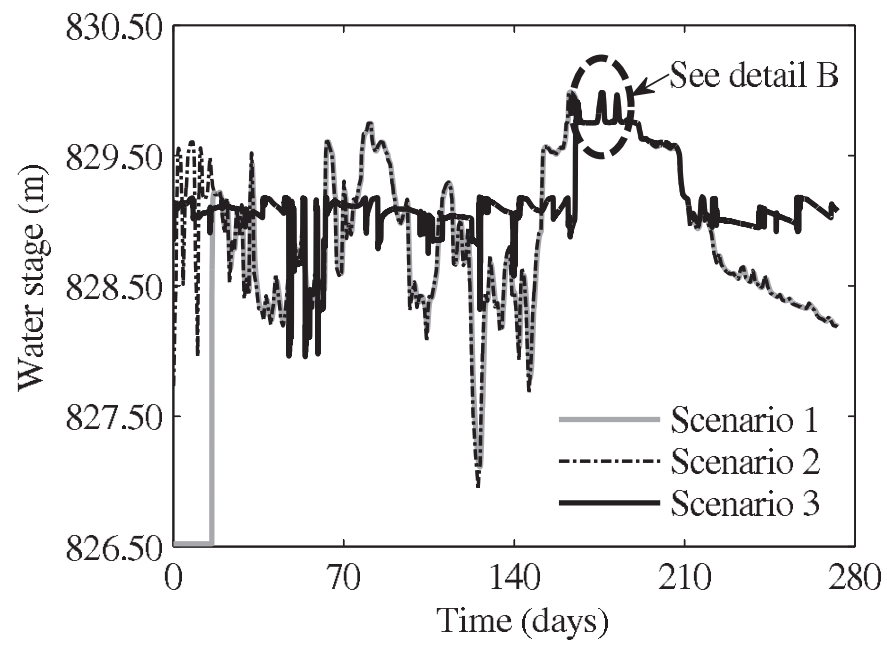


FIG. 19. Stage hydrographs at downstream end of reach R10 for simulated scenarios.

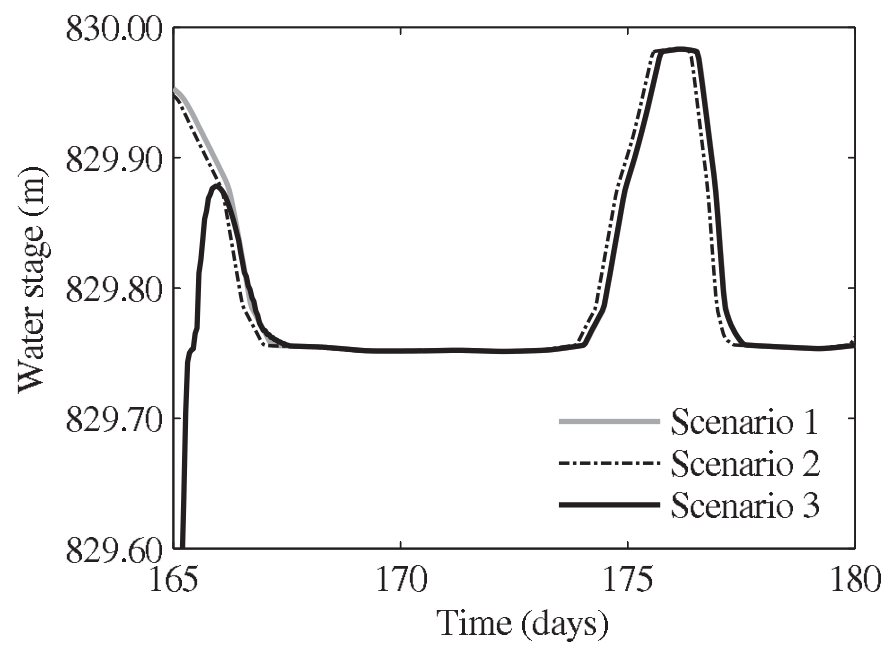


FIG. 20. Detail B in Figure 19.

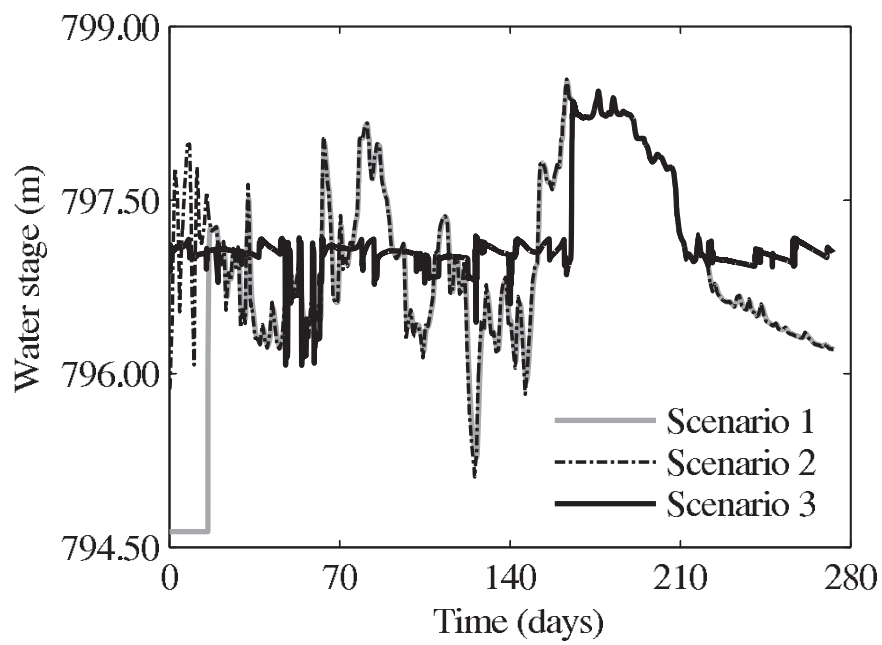


FIG. 21. Stage hydrographs at downstream end of reach R22 for simulated scenarios.

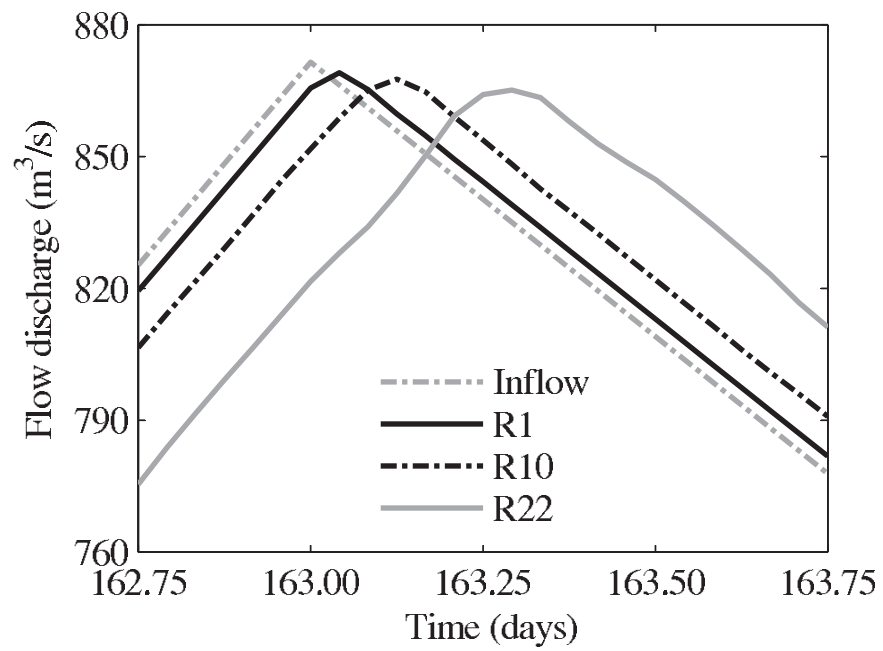


FIG. 22. Peak flow at downstream end of reaches R1, R10 and R22 for the second scenario.

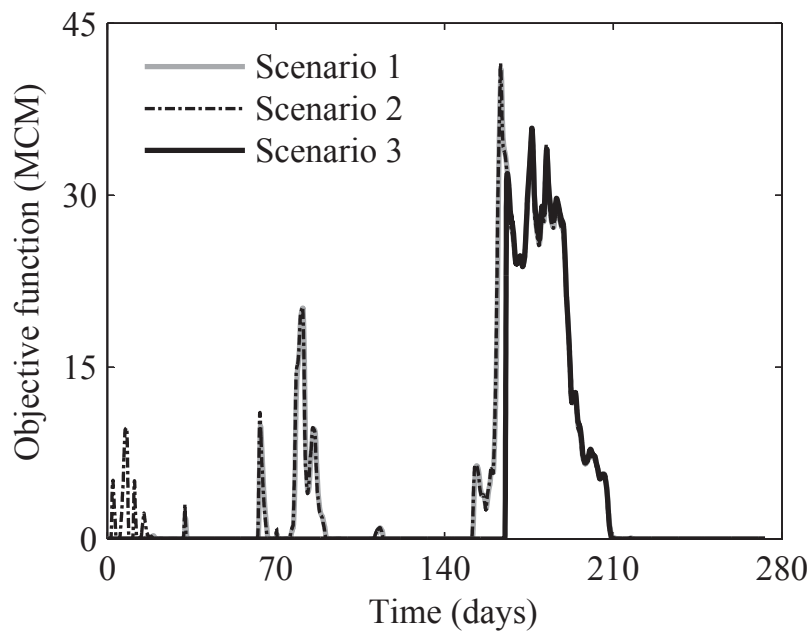


FIG. 23. Flooding objective (Eq. 1) for simulated scenarios.

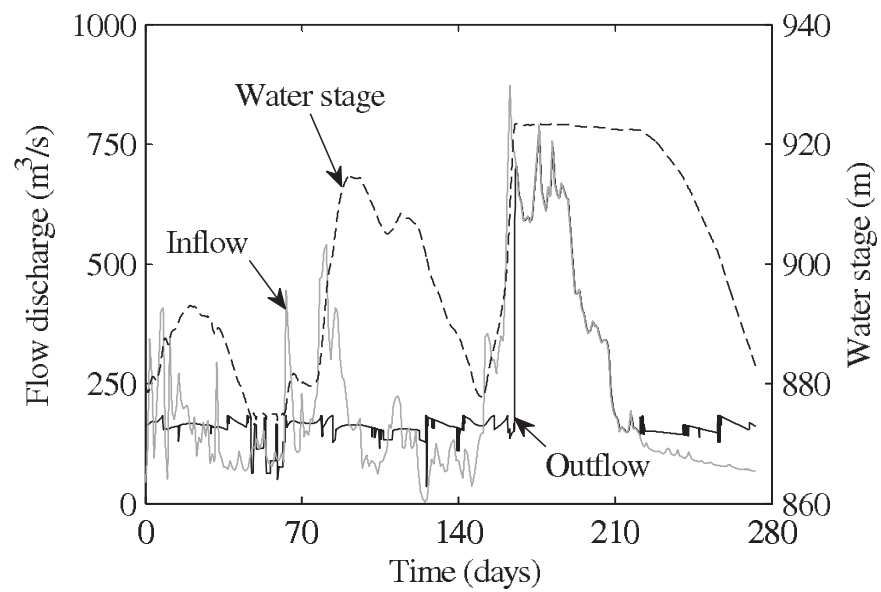


FIG. 24. Inflow, outflow and water stage hydrographs at the Lucky Peak reservoir.

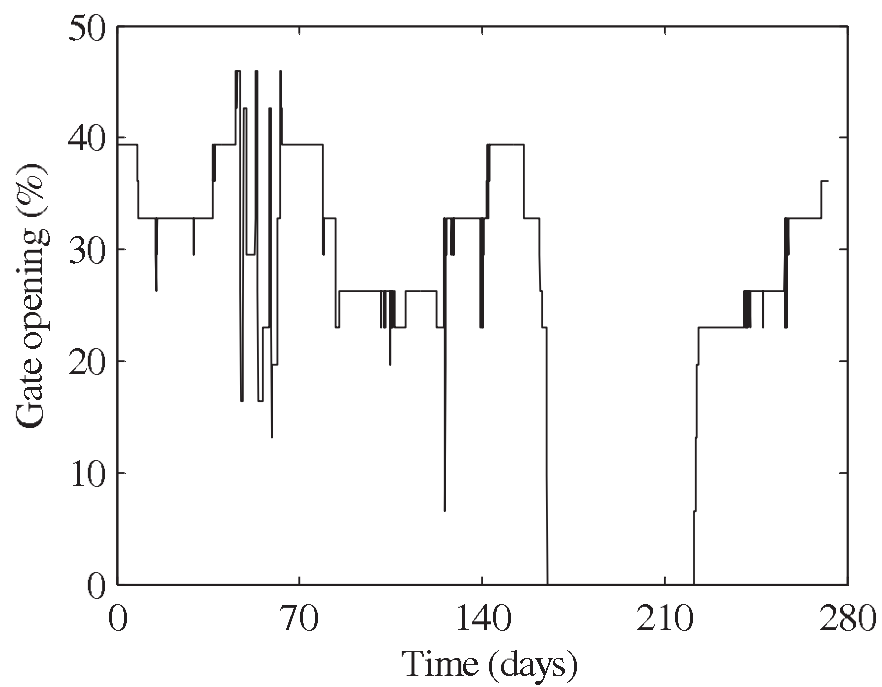


FIG. 25. Gate operation traces (six gates) at the Lucky Peak reservoir according to OSU Rivers

Reach ID	Upstream node	Downstream node	Length (m)	Upst. El. (z_u) (m)	Downst. El. (z_d) (m)	Slope (m/m)
R1	J1	J2	1043.77	847.38	846.48	0.000859
R2	J2	J3	1000.07	846.48	845.05	0.001428
R3	J3	J4	998.86	845.05	844.81	0.000244
R4	J4	J5	877.72	844.81	844.74	0.000082
R5	J5	J6	991.77	838.26	837.17	0.001098
R6	J6	J7	1049.35	837.17	835.81	0.001300
R7	J7	J8	1007.67	835.81	832.18	0.003604
R8	J8	J9	990.85	832.18	831.26	0.000922
R9	J9	J10	914.63	831.26	828.76	0.002736
R10	J10	J11	1051.12	828.76	826.50	0.002153
R11	J11	J12	857.98	826.50	824.08	0.002815
R12	J12	J13	918.46	824.08	821.42	0.002901
R13	J13	J14	1174.63	821.42	818.79	0.002235
R14	J14	J15	1025.32	818.79	815.31	0.003398
R15	J15	J16	1160.85	815.31	814.27	0.000893
R16	J16	J17	1082.18	812.89	810.29	0.002408
R17	J17	J18	1218.60	810.29	807.08	0.002636
R18	J18	J19	1067.34	807.08	804.87	0.002071
R19	J19	J20	1089.71	804.87	802.69	0.001996
R20	J20	J21	1069.99	802.70	800.07	0.002448
R21	J21	J22	984.18	800.07	797.31	0.002806
R22	J22	J23	971.03	797.31	794.60	0.002794
R23	J23	J24	1075.16	794.60	792.05	0.002369
R24	J24	J25	982.00	792.05	790.90	0.001172
R25	J25	J26	643.77	789.14	787.37	0.002750

TABLE 1. Characteristics of river reaches